

Supplementary Material for

## Topological ferroelectric nanostructures induced by mechanical strain in strontium titanate

Kairi MASUDA<sup>\*1</sup>, Le Van Lich<sup>\*2</sup>, Takahiro SHIMADA<sup>\*1</sup> and Takayuki KITAMURA<sup>\*1</sup>

<sup>\*1</sup> Department of Mechanical Engineering and Science, Kyoto University

Kyoto-daigaku-katsura, Nishikyo-ku, Kyoto 615-8540, Japan

<sup>\*2</sup> School of Materials Science and Engineering, Hanoi University of Science and Technology

No 1, Dai Co Viet Street, Hanoi, Viet Nam

### 1 Phase-Field modeling of SrTiO<sub>3</sub>

#### 1.1 Interactions of strain, polarization, and AFD in SrTiO<sub>3</sub>

Figure S1 shows the crystal structure of SrTiO<sub>3</sub>. Under the stress-free condition, the crystal structure is the perfect cubic structure as shown in Fig. S1(a). This cubic structure is called the paraelectric (PE) phase, and SrTiO<sub>3</sub> does not exhibit any spontaneous polarization. On the other hand, SrTiO<sub>3</sub> subject to tensile strain above a certain intensity exhibits spontaneous polarization along the tensile direction (Fig. S1(b))<sup>1-3</sup>. This structure is the ferroelectric (FE) phase with displacements of cations (Sr<sup>2+</sup>, Ti<sup>4+</sup>) and anions (O<sup>2-</sup>) from the ideal lattice positions. Thus, SrTiO<sub>3</sub> transforms from PE to FE by mechanical loading. Furthermore, at low temperature, SrTiO<sub>3</sub> exhibits the antiferrodistortive (AFD) phase, in which the oxygen octahedral rotates as shown in Fig. S1(c)<sup>4</sup>. The AFD and FE compete with each other<sup>5</sup>. Thus, strain, polarization, and AFD are coupled with each other in SrTiO<sub>3</sub>. To construct phase-field modeling of SrTiO<sub>3</sub>, these interactions must be incorporated into free energy.

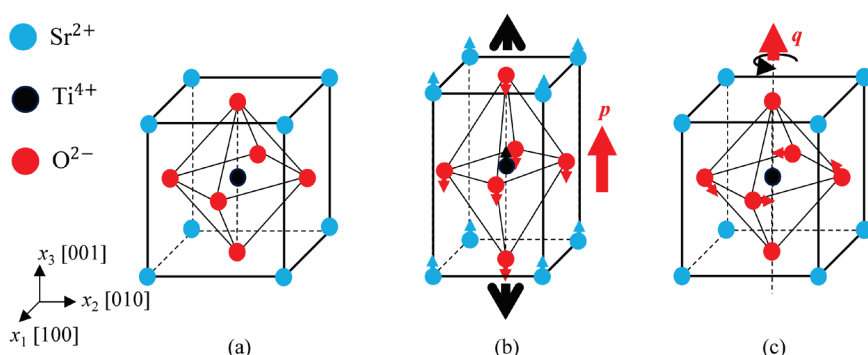


**Figure S1.** Crystal structures of SrTiO<sub>3</sub> (a) in the paraelectric phase, (b) in the ferroelectric phase under uniaxial strain along [001] and (c) in the AFD phase.

## 1.2 Free energy of SrTiO<sub>3</sub>

Taking polarization  $\mathbf{p} = (p_1, p_2, p_3)$  and AFD  $\mathbf{q} = (q_1, q_2, q_3)$  as the order parameters, the total free energy  $F$  can be shown as<sup>6–8</sup>

$$F = \int_V f dv = \int_V (f_{bulk} + f_{elas} + f_{grad} + f_{elec}) dv \quad (\text{S1})$$

where  $f$ ,  $f_{bulk}$ ,  $f_{elas}$ ,  $f_{grad}$ , and  $f_{elec}$  denote the total free energy density, the Landau energy density, the elastic energy density, the gradient free energy, and the electrostatic energy density.  $V$  denotes the entire volume of the SrTiO<sub>3</sub> system.

The Landau energy density  $f_{bulk}$  is expressed as

$$\begin{aligned} f_{bulk} = & \alpha_1(p_1^2 + p_2^2 + p_3^2) + \alpha_{11}(p_1^4 + p_2^4 + p_3^4) + \alpha_{12}(p_1^2 p_2^2 + p_2^2 p_3^2 + p_3^2 p_1^2) \\ & + \beta_1(q_1^2 + q_2^2 + q_3^2) + \beta_{11}(q_1^4 + q_2^4 + q_3^4) + \beta_{12}(q_1^2 q_2^2 + q_2^2 q_3^2 + q_3^2 q_1^2) \\ & - t_{11}(p_1^2 q_1^2 + p_2^2 q_2^2 + p_3^2 q_3^2) \\ & - t_{12}(p_1^2 (q_2^2 + q_3^2) + p_2^2 (q_3^2 + q_1^2) + p_3^2 (q_1^2 + q_2^2)) \\ & - t_{44}(p_1 p_2 q_1 q_2 + p_2 p_3 q_2 q_3 + p_3 p_1 q_3 q_1) \end{aligned} \quad (\text{S2})$$

where  $\alpha_I$ ,  $\alpha_{ij}$ ,  $\beta_I$ ,  $\beta_{ij}$  and  $t_{ij}$  are the Landau coefficients related to polarization, AFD and the coupling of polarization and AFD. The Landau energy density represents the property of polarization and AFD. Especially, the seventh, eighth and ninth term exhibit the coupling between polarization and AFD. The interaction of polarization and AFD is represented by these terms.

The elastic energy density is given by

$$f_{elas} = \frac{1}{2} c_{ijkl} e_{ij} e_{kl} = \frac{1}{2} c_{ijkl} (\varepsilon_{ij} - \varepsilon_{ij}^0)(\varepsilon_{kl} - \varepsilon_{kl}^0) \quad (\text{S3})$$

where  $c_{ijkl}$  denotes the elastic stiffness tensor.  $e_{ij}$  and  $\varepsilon_{ij}$  are an elastic strain and total strain, respectively.  $\varepsilon_{ij}^0$  is eigen-strain induced by polarization and AFD and shown as

$$\varepsilon_{ij}^0 = Q_{ijkl} p_k p_l + \Lambda_{ijkl} q_k q_l \quad (\text{S4})$$

where  $Q_{ijkl}$  and  $\Lambda_{ijkl}$  represent the electrostrictive coefficients and the coupling coefficients between strain and AFD, respectively. The expanded elastic energy density is given by

$$\begin{aligned}
f_{clas} = & \frac{1}{2} c_{11} (\varepsilon_{11}^2 + \varepsilon_{22}^2 + \varepsilon_{33}^2) + c_{12} (\varepsilon_{11}\varepsilon_{22} + \varepsilon_{22}\varepsilon_{33} + \varepsilon_{33}\varepsilon_{11}) + 2c_{44} (\varepsilon_{12}^2 + \varepsilon_{23}^2 + \varepsilon_{33}^2) \\
& - (c_{11}Q_{11} + 2c_{12}Q_{12})(\varepsilon_{11}p_1^2 + \varepsilon_{22}p_2^2 + \varepsilon_{33}p_3^2) \\
& - \{c_{11}Q_{12} + c_{12}(Q_{11} + Q_{12})\} \{ \varepsilon_{11}(p_2^2 + p_3^2) + \varepsilon_{22}(p_1^2 + p_3^2) + \varepsilon_{33}(p_1^2 + p_2^2) \} \\
& - 2c_{44}Q_{44} (\varepsilon_{12}p_1p_2 + \varepsilon_{23}p_2p_3 + \varepsilon_{13}p_1p_3) \\
& - (c_{11}\Lambda_{11} + 2c_{12}\Lambda_{12})(\varepsilon_{11}q_1^2 + \varepsilon_{22}q_2^2 + \varepsilon_{33}q_3^2) \\
& - \{c_{11}\Lambda_{12} + c_{12}(\Lambda_{11} + \Lambda_{12})\} \{ \varepsilon_{11}(q_2^2 + q_3^2) + \varepsilon_{22}(q_1^2 + q_3^2) + \varepsilon_{33}(q_1^2 + q_2^2) \} \\
& - 2c_{44}\Lambda_{44} (\varepsilon_{12}q_1q_2 + \varepsilon_{23}q_2q_3 + \varepsilon_{13}q_1q_3) \\
& + \frac{1}{2} \{c_{11}(Q_{11}^2 + 2Q_{12}^2) + 2c_{12}Q_{12}(2Q_{11} + Q_{12})\} (p_1^4 + p_2^4 + p_3^4) \\
& + \{c_{11}Q_{12}(2Q_{11} + Q_{12}) + c_{12}(Q_{11}^2 + 3Q_{12}^2 + 2Q_{11}Q_{12}) + 2c_{44}Q_{44}^2\} (p_1^2p_2^2 + p_2^2p_3^2 + p_3^2p_1^2) \\
& + \frac{1}{2} \{c_{11}(\Lambda_{11}^2 + 2\Lambda_{12}^2) + 2c_{12}\Lambda_{12}(2\Lambda_{11} + \Lambda_{12})\} (q_1^4 + q_2^4 + q_3^4) \\
& + \{c_{11}\Lambda_{12}(2\Lambda_{11} + \Lambda_{12}) + c_{12}(\Lambda_{11}^2 + 3\Lambda_{12}^2 + 2\Lambda_{11}\Lambda_{12}) + 2c_{44}\Lambda_{44}^2\} (q_1^2q_2^2 + q_2^2q_3^2 + q_3^2q_1^2) \\
& + [c_{11}(Q_{11}\Lambda_{11} + 2Q_{12}\Lambda_{12}) + 2c_{12}\{Q_{11}\Lambda_{12} + Q_{12}(\Lambda_{11} + \Lambda_{12})\}] (p_1^2q_1^2 + p_2^2q_2^2 + p_3^2q_3^2) \\
& + [c_{11}\{Q_{11}\Lambda_{12} + Q_{12}(\Lambda_{11} + \Lambda_{12})\} + c_{12}\{(Q_{11} + Q_{12})(\Lambda_{11} + \Lambda_{12}) + 2Q_{12}\Lambda_{12}\}] \\
& \{p_1^2(q_2^2 + q_3^2) + p_2^2(q_3^2 + q_1^2) + p_3^2(q_1^2 + q_2^2)\} \\
& + 4c_{44}Q_{44}\Lambda_{44} (p_1p_2q_1q_2 + p_2p_3q_2q_3 + p_3p_1q_3q_1)
\end{aligned} \tag{S5}$$

where, following the Voigt notation,  $c_{11} = c_{1111}$ ,  $c_{12} = c_{1122}$ ,  $c_{44} = c_{1212}$ ,  $Q_{11} = Q_{1111}$ ,  $Q_{12} = Q_{1122}$ ,  $Q_{44} = Q_{1212}/2$ ,  $\Lambda_{11} = \Lambda_{1111}$ ,  $\Lambda_{12} = \Lambda_{1122}$  and  $\Lambda_{44} = \Lambda_{1212}/2$ , respectively. Especially, the fourth, fifth and sixth term exhibit the coupling between polarization and strain. The interaction of polarization and strain is represented by these terms.

The gradient energy density, which is the penalty for the spatially inhomogeneous order parameters, is described as

$$\begin{aligned}
f_{glad} = & \frac{1}{2} G_p (p_{1,1}^2 + p_{1,2}^2 + p_{1,3}^2 + p_{2,1}^2 + p_{2,2}^2 + p_{2,3}^2 + p_{3,1}^2 + p_{3,2}^2 + p_{3,3}^2) \\
& + \frac{1}{2} G_q (q_{1,1}^2 + q_{1,2}^2 + q_{1,3}^2 + q_{2,1}^2 + q_{2,2}^2 + q_{2,3}^2 + q_{3,1}^2 + q_{3,2}^2 + q_{3,3}^2)
\end{aligned} \tag{S6}$$

where  $G_p$  and  $G_q$  are the gradient coefficients related to polarization and AFD, respectively.  $p_{i,j} = \delta p_i / \delta x_j$  and  $q_{i,j} = \delta q_i / \delta x_j$  are gradients of polarization and AFD using the position vector  $\mathbf{x} = (x_1, x_2, x_3)$ .

The electrostatic energy density is given as

$$f_{elec} = -\frac{1}{2}\varepsilon_0(\kappa_{11}E_1^2 + \kappa_{22}E_2^2 + \kappa_{33}E_3^2) - (E_1p_1 + E_2p_2 + E_3p_3) \quad (S7)$$

where,  $E_i$ ,  $\varepsilon_0$  denote electric field components, the permittivity of vacuum.  $\kappa_{ij}$  is the relative dielectric permittivity of SrTiO<sub>3</sub>.

The total free energy mentioned above includes the interactions of strain, polarization, and AFD, which are essential to describe the properties of SrTiO<sub>3</sub>.

### 1.3 Governing equations in SrTiO<sub>3</sub>

The temporal and spatial evolution of polarization and AFD are calculated by the time-dependent Ginzburg-Landau (TDGL) equations,

$$\frac{\partial p_i(\mathbf{x}, t)}{\partial t} = -L_p \frac{\delta F}{\delta p_i(\mathbf{x}, t)} \quad (S8)$$

$$\frac{\partial q_i(\mathbf{x}, t)}{\partial t} = -L_q \frac{\delta F}{\delta q_i(\mathbf{x}, t)} \quad (S9)$$

where  $t$  represents time.  $L_p$  and  $L_q$  are the kinetic coefficients related to the domain mobility for polarization and AFD, respectively.  $\delta F/\delta p_i$  and  $\delta F/\delta q_i$  denote the thermodynamic driving forces for polarization and AFD evolution. In addition to the time-dependent Ginzburg-Landau equations, the following mechanical equilibrium equation

$$\frac{\partial}{\partial x_j} \left( \frac{\partial f}{\partial \varepsilon_{ij}} \right) = 0 \quad (S10)$$

and Maxwell-Gauss equation

$$\frac{\partial}{\partial x_i} \left( -\frac{\partial f}{\partial E_i} \right) = 0 \quad (S11)$$

must be satisfied for charge and body force free ferroelectric materials simultaneously.

Using the principle of virtual work, the governing equations are expressed in the weak form as

$$\begin{aligned} & \int_V \left\{ \frac{\partial f}{\partial \varepsilon_{ij}} \delta \varepsilon_{ij} + \frac{\partial f}{\partial E_i} \delta E_i + \frac{\partial f}{\partial p_{i,j}} \delta p_{i,j} + \frac{\partial f}{\partial p_i} \delta p_i + \frac{\partial f}{\partial q_{i,j}} \delta q_{i,j} + \frac{\partial f}{\partial q_i} \delta q_i \right\} dV \\ &= \int_S \left\{ t_i \delta u_i - \omega d\varphi + \frac{\partial f}{\partial p_{i,j}} n_j \delta p_i + \frac{\partial f}{\partial q_{i,j}} n_j \delta q_i \right\} dS \end{aligned} \quad (S12)$$

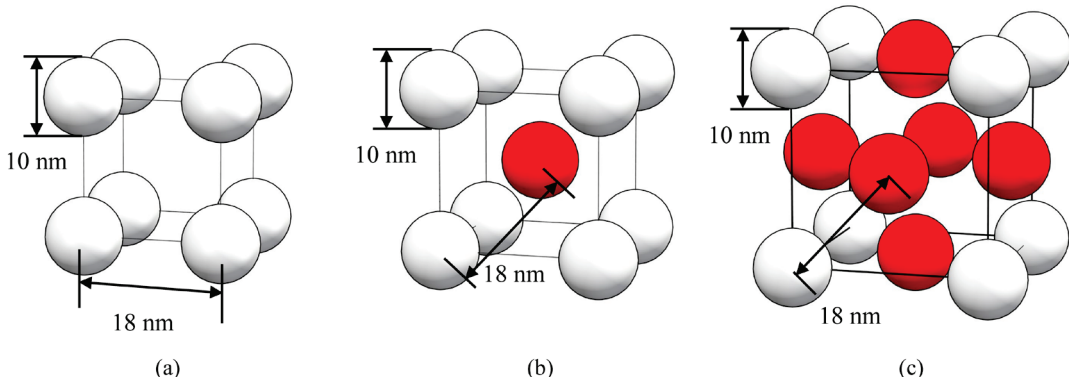
where  $t_i$ ,  $u_i$ ,  $\omega$ ,  $\varphi$ ,  $n_j$  and  $S$  denote the surface traction, displacements, surface charge, electric potential, the normal vector of surface and the surface of materials.

## 2 Simulation models

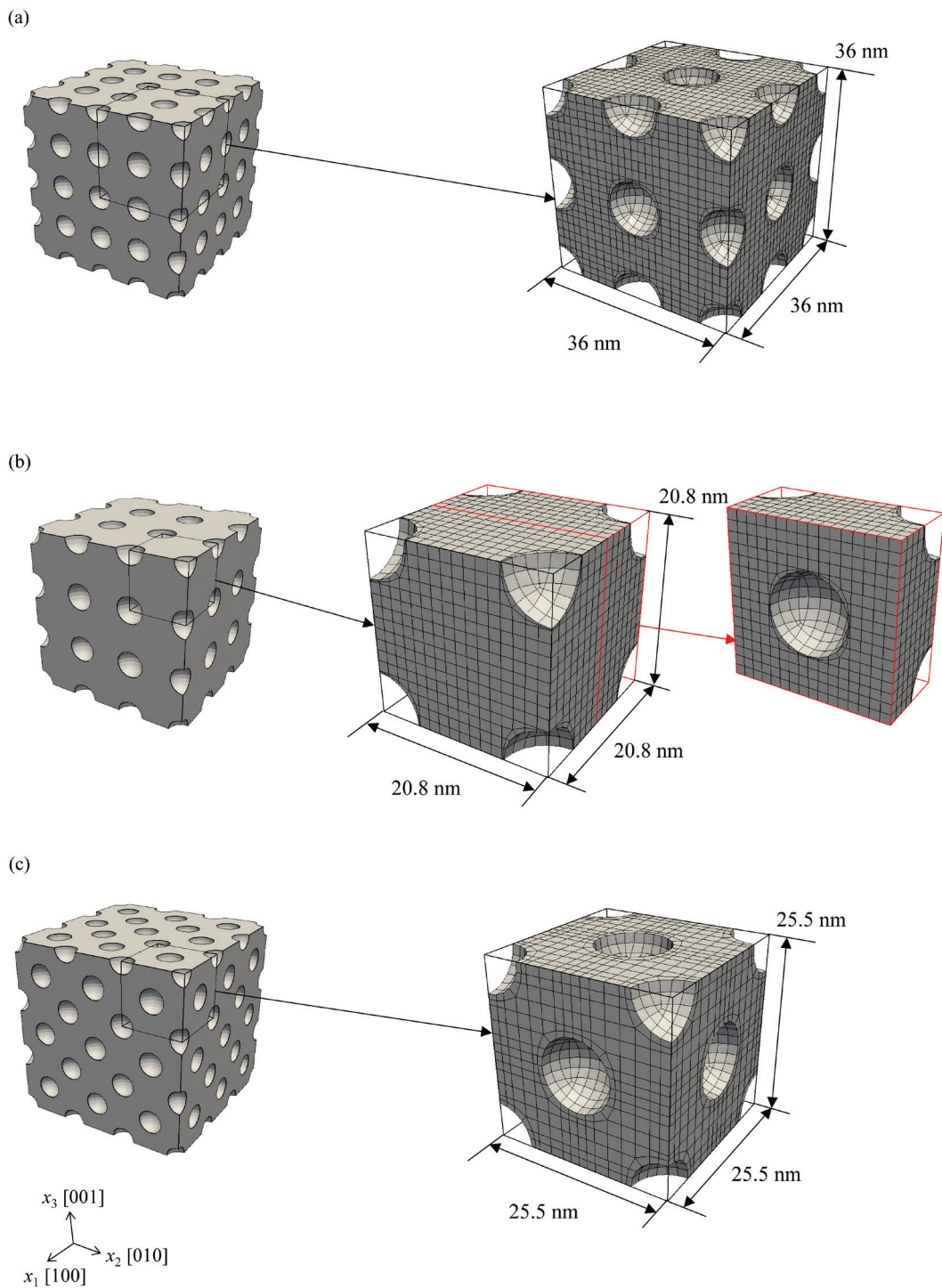
Figure S2 shows pore arrangements in nanoporous SrTiO<sub>3</sub>. To study the effect of pore arrangements, I employ simple-cubic (SC), body-centered cubic (BCC) and face-centered cubic (FCC) arrangements of spherical pores. On the basis of the experimental observations<sup>9,10</sup>, the diameter of a pore and the nearest distance between pores are 10 nm and 18 nm, respectively.

Figure S3(a) shows the simulation model of the SC nanoporous SrTiO<sub>3</sub>. The model consists of a single crystal of SrTiO<sub>3</sub> in which the crystal orientation [100], [010] and [001] corresponds to the  $x_1$ ,  $x_2$  and  $x_3$  axis of the model. The size of the simulation cell in the  $x_1$ ,  $x_2$  and  $x_3$  directions is 36 nm×36 nm×36 nm, and this simulation cell is divided into 13824 elements with 16338 nodes. The periodic boundary condition is applied to the simulation cell in the  $x_1$ ,  $x_2$  and  $x_3$  directions to realize the SC nanoporous structure. The electric boundary conditions are set to be open-circuited to mimic the free-surface condition via taken into account the depolarization field which is derived from surface charges. The values of the material coefficients for SrTiO<sub>3</sub> are given in Table S1<sup>6,11</sup>.

Figures S3(b) and S3(c) show the simulation models of BCC and FCC nanoporous SrTiO<sub>3</sub>. Same as SC nanoporous SrTiO<sub>3</sub>, the models consist of a single crystal of SrTiO<sub>3</sub> in which the crystal orientation [100], [010] and [001] corresponds to the  $x_1$ ,  $x_2$  and  $x_3$  axis. The size of the simulation cells of BCC and FCC structures in the  $x_1$ ,  $x_2$  and  $x_3$  directions are 20.8 nm×20.8 nm×20.8 nm and 25.5 nm×25.5 nm×25.5 nm, respectively. These simulation cells are divided into 4096 elements with 5086 nodes and 4096 elements with 5269 nodes. The periodic boundary conditions are applied to each simulation cells in the  $x_1$ ,  $x_2$  and  $x_3$  directions to realize BCC and FCC nanoporous structures. The electric boundary conditions and the values of the material coefficients are the same as SC nanoporous structure.



**Figure S2.** The pore arrangements investigated in this study. (a) SC, (b) BCC and (c) FCC.



**Figure S3.** Simulation models of (a) SC, (b) BCC and (c) FCC nanoporous and its dimensions and mesh partition.

**Table S1 Material constants for SrTiO<sub>3</sub> used in the simulation**

Landau coefficients for polarization		Landau coefficients for AFD	
$\alpha_1$ [dyn cm <sup>2</sup> /stac <sup>2</sup> ]	$4.5 \times 10^{-3} [\coth(54/T) - \coth(54/30)]$	$\beta_1$ [dyn/cm <sup>4</sup> ]	$1.32 \times 10^{26} [\coth(145/T) - \coth(145/105)]$
$\alpha_{11}$ [dyn cm <sup>6</sup> /stac <sup>4</sup> ]	$2.1 \times 10^{-12}$	$\beta_{11}$ [dyn/cm <sup>6</sup> ]	$1.69 \times 10^{43}$
$\alpha_{12}$ [dyn cm <sup>6</sup> /stac <sup>4</sup> ]	$4.85 \times 10^{-12}$	$\beta_{12}$ [dyn/cm <sup>6</sup> ]	$3.88 \times 10^{43}$
Coupling coefficients for polarization		Coupling coefficient for AFD	
$Q_{11}$ [cm <sup>4</sup> /stac <sup>2</sup> ]	$5.09 \times 10^{-13}$	$A_{11}$ [/cm <sup>2</sup> ]	$8.7 \times 10^{14}$
$Q_{12}$ [cm <sup>4</sup> /stac <sup>2</sup> ]	$-1.50 \times 10^{-13}$	$A_{12}$ [/cm <sup>2</sup> ]	$-7.8 \times 10^{14}$
$Q_{44}$ [cm <sup>4</sup> /stac <sup>2</sup> ]	$1.065 \times 10^{-13}$	$A_{44}$ [/cm <sup>2</sup> ]	$-9.2 \times 10^{14}$
Elastic constants		Relative gradient constants	
$c_{11}$ [dyn/cm <sup>2</sup> ]	$3.36 \times 10^{12}$	$G_p/G_0$	0.4
$c_{12}$ [dyn/cm <sup>2</sup> ]	$1.07 \times 10^{12}$	$G_q/G_p$	0.012
$c_{44}$ [dyn/cm <sup>2</sup> ]	$1.27 \times 10^{12}$	Relative dielectric constant	
		$\kappa$	300

### 3 Simulation procedure

To investigate the behavior of polarization distributions under tensile strain, at first, the thermodynamic equilibrium state of nanoporous SrTiO<sub>3</sub> without external strain is simulated. The simulation is conducted at room temperature ( $T = 300$  K) and SrTiO<sub>3</sub> does not show AFD which appears at low temperature ( $T = 105$  K). To obtain the thermodynamic equilibrium state, a random distribution of polarization with small magnitude  $1 \times 10^{-5}$  C/m<sup>2</sup> is introduced as the initial state. The time evolution of polarization is calculated by solving the TDGL equation until the change of polarization at each time step becomes less than  $1 \times 10^{-6}$  C/m<sup>2</sup>. For the time integration and nonlinear iteration, the backward Euler scheme and the Newton iteration method are used respectively with normalized time step  $\Delta t/t_0 = 0.2$  ( $t_0 = L_p |\alpha_1|$ ).

Next, a small equitriaxial tensile strain  $\Delta \varepsilon_{11} = \Delta \varepsilon_{22} = \Delta \varepsilon_{33} = 0.001$  is applied to nanoporous SrTiO<sub>3</sub> simulated above, and the thermodynamic equilibrium state is simulated in the same manner as that without external strain. By repeating small increments of strain and calculating the thermodynamic equilibrium state, we study the behavior of polarization distributions in nanoporous SrTiO<sub>3</sub> under tensile strain.

## 4 Strain distributions

Figure S4 shows the strain distribution in nanoporous SrTiO<sub>3</sub> under triaxial strain  $\varepsilon_{\text{global}}$  by using the finite element method (FEM). The model and the elastic coefficients are the same as Fig. S3 and Table S1. Noted that, to represent the complicated strain distribution in nanoporous materials, we use the equivalent strain shown as<sup>12</sup>

$$\varepsilon_{\text{eq}} = \frac{\sqrt{2}}{3} \left[ (\varepsilon_{11} - \varepsilon_{22})^2 + (\varepsilon_{22} - \varepsilon_{33})^2 + (\varepsilon_{33} - \varepsilon_{11})^2 + \frac{3}{2}(\varepsilon_{12}^2 + \varepsilon_{23}^2 + \varepsilon_{31}^2) \right]^{1/2}, \quad (\text{S13})$$

where  $\varepsilon_{ij}$  are strain tensor. Furthermore, to exhibit the expanding direction of strain intensity, we show the isosurface of the equivalent strain  $\varepsilon_{\text{eq}} = 0.023$  as strain distributions.

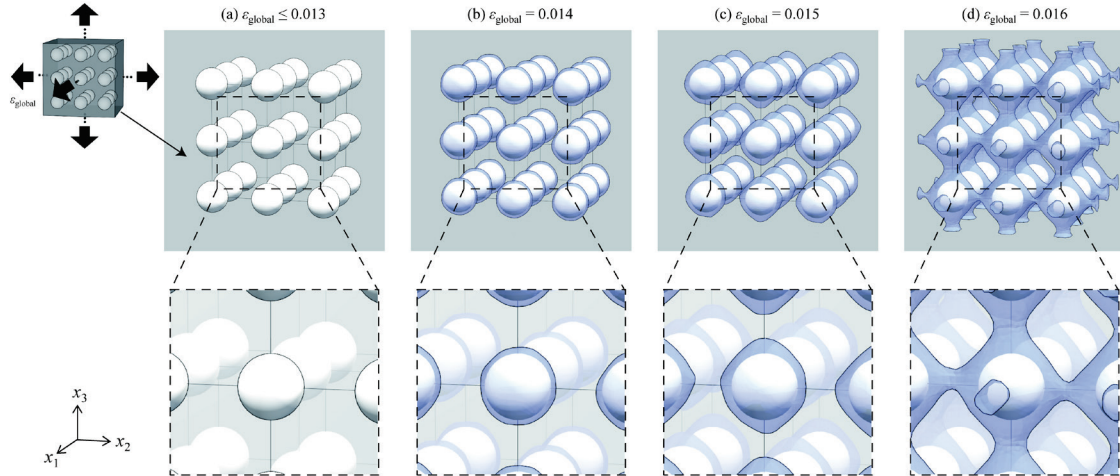


**Figure S4.1** Strain distributions of SC nanoporous SrTiO<sub>3</sub> under triaxial strain. The blue region indicates the isosurface of equivalent strain  $\varepsilon_{\text{eq}} = 0.023$ .

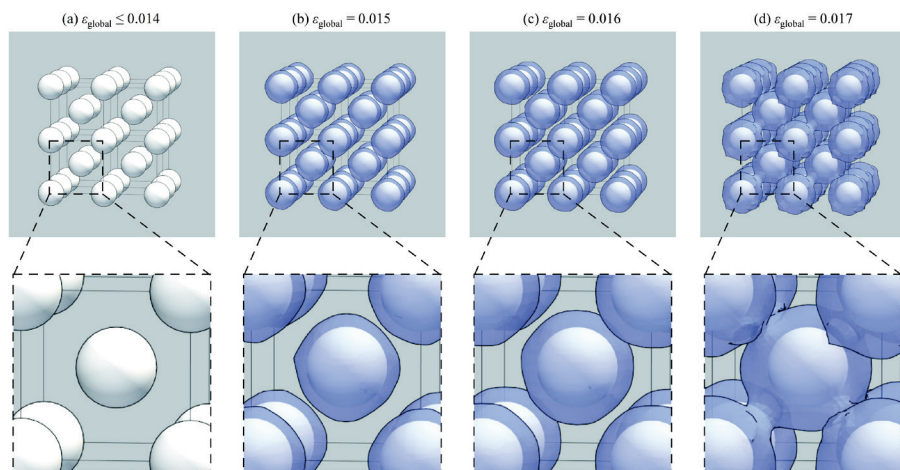


**Figure S4.2** Strain distributions of BCC nanoporous SrTiO<sub>3</sub> under triaxial strain.

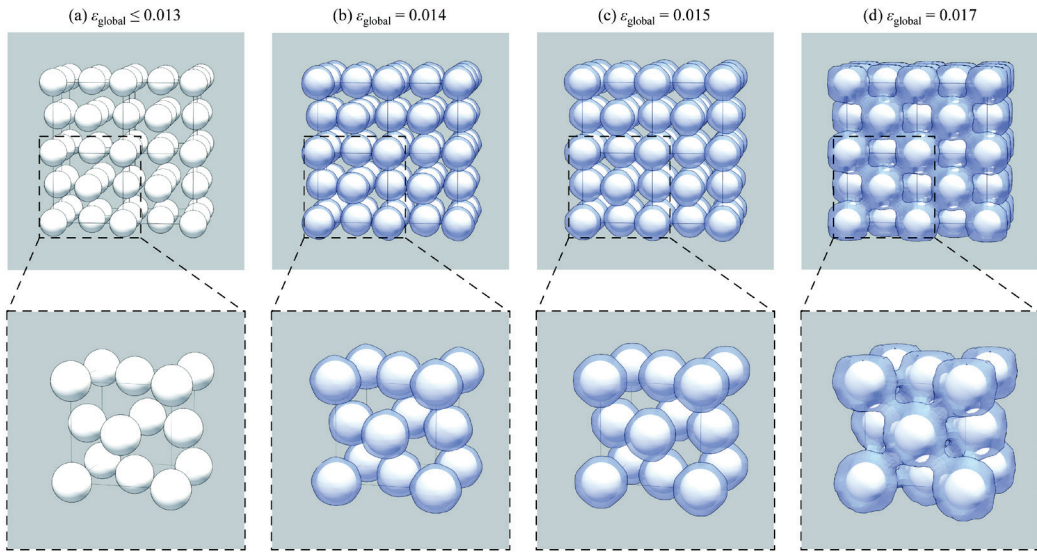


**Figure S4.3** Strain distributions of FCC nanoporous SrTiO<sub>3</sub> under triaxial strain.

## Reference

- 1 H. Uwe and T. Sakudo, *Phys. Rev. B*, 1976, **13**, 271–286.
- 2 J. H. Haeni, P. Irvin, W. Chang, R. Uecker, P. Reiche, Y. L. Li, S. Choudhury, W. Tian, M. E. Hawley, B. Craig, A. K. Tagantsev, X. Q. Pan, S. K. Streiffer, L. Q. Chen, S. W. Kirchoefer, J. Levy and D. G. Schlom, *Nature*, 2004, **430**, 758–761.
- 3 A. Vasudevarao, A. Kumar, L. Tian, J. H. Haeni, Y. L. Li, C. J. Eklund, Q. X. Jia, R. Uecker, P. Reiche, K. M. Rabe, L. Q. Chen, D. G. Schlom and V. Gopalan, *Phys. Rev. Lett.*, 2006, **97**, 257602.
- 4 H. Unoki and T. Sakudo, *J. Phys. Soc. Jpn.*, 1967, **23**, 546–552.
- 5 U. Aschauer and N. A. Spaldin, *J. Phys. Condens. Matter*, 2014, **26**, 122203.
- 6 G. Sheng, Y. L. Li, J. X. Zhang, S. Choudhury, Q. X. Jia, V. Gopalan, D. G. Schlom, Z. K. Liu and L. Q. Chen, *J. Appl. Phys.*, 2010, **108**, 084113.
- 7 G. Sheng, Y. L. Li, J. X. Zhang, S. Choudhury, Q. X. Jia, V. Gopalan, D. G. Schlom, Z. K. Liu and L. Q. Chen, *Appl. Phys. Lett.*, 2010, **96**, 232902.
- 8 Y. L. Li, S. Choudhury, J. H. Haeni, M. D. Biegalski, A. Vasudevarao, A. Sharan, H. Z. Ma, J. Levy, V. Gopalan, S. Trolier-McKinstry, D. G. Schlom, Q. X. Jia and L. Q. Chen, *Phys. Rev. B*, 2006, **73**, 184112.
- 9 E. J. W. Crossland, N. Noel, V. Sivaram, T. Leijtens, J. A. Alexander-Webber and H. J. Snaith, *Nature*, 2013, **495**, 215–219.
- 10 D. Gross, C. Boissière, B. Smarsly, T. Brezesinski, N. Pinna, P. A. Albouy, H. Amenitsch, M. Antonietti and C. Sanchez, *Nat. Mater.*, 2004, **3**, 787–792.
- 11 B. K. Choudhury, K. V. Rao and R. N. P. Choudhury, *J. Mater. Sci.*, 1989, **24**, 3469–3474.
- 12 R. V. Mises, *Götting. Nachr. Math. Phys.*, 1913, **1**, 582–592.